ANALYTIC PROPERTIES OF TRANSITION AMPLITUDES

Peter Vincent Landshoff

St. John's College, Cambridge

and

Palmer Physical Laboratory, Princeton University

A dissertation for the Degree of Doctor of Philosophy at the University of Cambridge

March, 1962

This is an account of original work. A large part of it was performed in collaboration and most of it has been described in references (1) to (8). No part of the dissertation has been submitted for any degree or diploma at any other university, and no part is being submitted for any such degree or diploma.

I wish to thank all those with whom I have worked for their kind cooperation. Their names appear in the list of references. In particular, I take this opportunity of expressing my gratitude to Dr. J. C. Polkinghorne for his stimulating guidance during the first two years of my research and to Dr. M. L. Goldberger for the hospitality of the Physics Department of Princeton University in the third year.

I gratefully acknowledge the support of a Slater Studentship, the Amy Mary Preston Read Scholarship, a D.S.I.R. Studentship, a St. John's College Research Fellowship, the U.S.A.F. and a Fulbright grant.

P. V. Landshoff

CONTENTS

INTRODUCTION

Early work in elementary particle physics was concerned with electrodynamics, that is with interactions involving only electrons and photons. Here one can use a Lagrangian or a Hamiltonian which is exactly similar to its counterpart in classical physics. An integral equation for transition amplitudes may then be obtained. This may be solved formally and yield an infinite series in powers of the coupling constant, which is a measure of the strength of the interaction. There is a difficulty in that each term of the series, the perturbation series, consists of a divergent integral. However, a physically plausible prescription may be given for separating out the infinities and then, since the electrodynamic coupling constant is small, there is a hope that the remaining series converges, at least asymptotically. Calculations of the electron magnetic moment and of the Lamb shift using the first few terms of the series give results in miraculously close agreement with experiment.

For interactions involving other particles the situation is much less satisfactory. Classical analogy is now of little help in suggesting the nature of the interaction. Even if a plausible guess is made the perturbation series then derived has negligible change

of being convergent since the interaction is strong and therefore the coupling constant is large (We do not discuss here the weak interactions. In the context of these even the concept of a particle is at present ill-defined).

For the last six years, therefore, the tendency has been to try a different approach. One inserts no details of the nature of the interaction into the theory, but only assumes some general principles which surely cannot be violated in any local field theory. The usual basic axioms are:

(i) Invariance of the theory under transformations of the proper Poincaré group, so that the requirements of special relativity are satisfied.

(ii) The absence of states of negative energy and the uniqueness of the vacuum state. The concept of energy follows as a result of the translation invariance that is implied by the first axiom.

(iii)Two boson field operators commute when their arguments have spacelike separation. Fermion field operators anticommute. This is generally supposed to be in some way equivalent to the requirements of causality.

(iv) The square of the norm of a state vector in the Hilbert space of the field operators is non-negative. This implies that there exists no states occurring with negative probability and is a non-trivial requirement since such states are found in simple models that have been constructed.

(v) In the remote past and the remote future the fields behave as free fields. This corresponds to the fact that in an experiment the particles involved are so far apart when they are actually observed that the interactions between them are negligible. Problems in this connection arise in the case of bound states.

A suitable mathematical expression of the last axiom implies the existence of a unitary operator whose matrix element between state vectors is the transition amplitude. Matrix elements occurring in the theory must be regarded as distributions and it is hoped that they are temperate.

Simple heuristic arguments lead one to suppose that the axioms imply the possibility of expressing transition amplitudes as the real boundary values of analytic functions of several complex variables. Such functions then relate together values of a given transition amplitude at different energies and momentum transfers. Also, since there may be several

different boundary values according to how and where the limit on the real boundary is taken, there arises the possibility of relating together matrix elements corresponding to apparently distinct physical processes as different boundary values of the same analytic function.

If the holomorphy domain of the complex function is suitably large an application of the Cauchy formula or of the Bergmann-Weyl formula yields an integral equation, a dispersion relation, which may be of practical value. In fact, dispersion relations have been very widely used in the reduction of experimental data, though very few have actually been proved to be valid.

Unfortunately, the problem of the computation of the holomorphy domain is one of supreme difficulty. The first three axioms result in the required domain being the holomorphy envelope of a most complicated initial domain and the analytic completion has so far only been performed for the three-point function[9]. No means have yet been found for incorporating the consequences of the other axioms, nor the fact that the values of the masses of the elementary particles form a set of discrete numbers.

Therefore, to obtain guidance on the general problem, attention has been given to the analytic

properties of the terms of the perturbation series. This means, of course, that some details of the interaction are assumed, but all that is necessary is that the Hamiltonian be a polynomial in the field operators and a finite number of their derivatives. As it is so unlikely that the perturbation series converges one might be sceptical of the usefulness of deriving the analytic properties of its individual terms, even though these properties be common to all terms. However, the results obtained are convincingly reasonable physically, and in very good agreement with the limited results of general theory[9]. For example, anomalous thresholds were first discovered in perturbation theory[10]. Their presence in the general theory has since been confirmed and they are recognised as being an inevitable consequence of physics.

Recently a different philosophy has been developed. Because dispersion relations have proved to be of practical value and because it is not even certain that there is any local field theory that satisfies the axioms, it is proposed that field theory be discarded and that the basic axioms be concerned directly with the analyticity properties of the transition amplitudes*. It is proposed that the domain of holomorphy be, in some sense,

---

* This philosophy has been favoured particularly by G.F. Chew

as large as possible consistent with the unitarity requirements associated with conservation of probability. It has been shewn[11] that this restriction demands at least the presence of the singularities of perturbation theory, so that with this approach it is again useful to investigate the analytic properties of perturbation theory.

In Chapter 1 are described the methods for determining the positions of the possible singularities of the Feynman integrals that are the terms of a perturbation expansion. These methods are based on the generalisation of a lemma of Hadamard[12]. The positions are found, in principle, by solving a set of simultaneous equations known as the Landau equations. In practice, it is too difficult to solve these equations algebraically except in the simplest cases and a geometrical method is used. This method is known as the dual diagram analysis[13]. The original form of the dual diagram analysis is found, however, to omit a large class of solutions of the Landau equations. These new solutions are known as second-type solutions.

The analytic functions of which the transition

amplitudes are the boundary values have singularities to which must be attached cuts, so that the functions have many Riemann sheets. The dispersion relations that have been conjectured demand analyticity on only one of these sheets, called the physical sheet. Hence once the positions of the perturbation theory singularities have been found, as is described in Chapter 1, it is necessary to decide which singularities are present on the physical sheet. A discussion of this question is taken up in Chapter 2.

Chapter 3 deals with the application of some of the techniques to production reactions, in which two particles come in and more than two emerge. It is found that there are singularities whose presence is a severe embarrassment in that they invalidate simple dispersion relations. This is unfortunate in that it seems to make even more difficult than one would hope the task of evaluating the contributions, implied by the unitarity condition, to the ordinary two-particle two-particle scattering amplitude from many-particle intermediate states. The singularities may also upset certain extrapolations from experimental data for production processes. These are performed to obtain information about simple scattering processes which

themselves cannot be conveniently performed in the laboratory. Under certain conditions the singularities can come so close to the boundary of complex variable space at which the physical value of the production amplitude is calculated that they may be expected to produce an effect that could be directly observed experimentally. Some examples are given of when this might occur, but none represents an experiment that is easily performed at present.

1. Positions of Singularities

1.1 The Landau equations

A given term in a perturbation series may be represented by a Feynman graph. The corresponding contribution to the transition amplitude is a multiple integral

$$I = \int_{-\infty}^{\infty} \prod_j d^4\vec{k}_j \int_0^1 \prod_{i=1}^{N} d\alpha_i \; \frac{\nu\, \delta(\Sigma\alpha_i - 1)}{\psi^N} \qquad (1)$$

where*

$$\psi(\vec{p}, \vec{k}, \alpha) = \sum_i \alpha_i (\vec{q}_i^{\,2} - m_i^2) \qquad (2)$$

Here $\vec{q}_i, m_i$ are respectively the momentum 4-vector and the mass associated with the i^{th} internal line of the graph, there being N such lines. Each line has an integration parameter α_i associated with it. A set of independent closed loops is chosen in the graph and the integration variable $\vec{k}_j$ is the 4-momentum running round the j^{th} such loop. The integral I is a function of the scalar products of the external vectors $\vec{p}$ for the graph. The function ν is a polynomial in the $\vec{q}_i$, the m_i and the

* Arrows above quantities denote that they are vectors in Lorentz space.

Dirac γ-matrices. It is usually supposed that its precise form has no effect on the analytic properties of the integral, so that it suffices to take $\nu \equiv 1$, although under certain conditions this is not the case.

In principle it is possible to investigate the analytic properties of $I(z)$ by performing the integrations involved and examining the resulting function. However, even for the fourth order scattering graph this function is prohibitively complicated, being the sum of one hundred and ninety-two Spence functions[15]. It is therefore necessary to find a better method. Hadamard gave such a method for the case of a single integration[12] and we shall generalise this to our multi-dimensional integral.

The integration is over a "hypercontour" A in real (k,α) - space and I is evidently regular when the z are such that the manifold $\psi = 0$ does not intersect A. A consequence of Cauchy's theorem is that when it does intersect A an analytic continuation of I is provided by distorting A into the complex (k,α) - space so as to avoid $\psi = 0$. The possibility of this

distortion can only cease when the manifold ψ degenerates and becomes locally cone-like, the hypercomtour A being pinched between the two parts of ψ at the vertex of the cone. The necessary conditions for this are the Hadamard equations:

$$\frac{\partial \psi}{\partial \vec{k}_j} = 0 \tag{3}$$

for each j and

$$\frac{\partial \psi}{\partial \alpha_i} = 0 \tag{4}$$

for each i.

Singularities of this type are known as <u>leading</u> singularities of the graph. There are additional singularities arising from the fact that the distortions of the edge of the hypercontour are restricted to the analytic manifolds on which one of the α vanishes, the edges of the edges are restricted to those manifolds on which two α vanish, etc. These are the <u>lower-order</u> singularities for which (4) is replaced by the condition $\alpha_i = 0$ for one or more i. They are the leading singularities for the graphs obtained from the original graphs by contracting

the corresponding internal lines.

From the explicit expression (2) for ψ we see that (3) and (4) are equivalent to

$$\sum_j \alpha_i \vec{q}_i = 0 \qquad \text{for each } j \qquad (5)$$

and

$$\vec{q}_i^{\,2} = m_i^2 \qquad \text{for each } i \qquad (6)$$

where, in (5), Σ_j indicates summation round the j^{th} closed loop of the graph. These two sets of equations are the Landau equations.

The integration over the k_j in (1) may be simply performed. We write ψ in the form

$$\psi(\vec{p}, \vec{k}, \alpha) = \vec{k}^T \underline{A} \vec{k} - 2\vec{k}^T \underline{B} \vec{p} + (\vec{p}^T \underline{\Gamma} \vec{p} - \sigma) \qquad (7)$$

where $\sigma = \Sigma_i \alpha_i m_i^2$. Here $\underline{A}$, $\underline{B}$, $\underline{\Gamma}$ are respectively $L \times L$, $L \times (E-1)$ and $(E-1) \times (E-1)$ matrices whose elements are linear combinations of the α. L is the number of independent loops in the graph and in (7) there enter (E - 1) independent vectors $\vec{p}$, the last of the E external vectors being expressible in terms of the others because of energy-

momentum conservation. Underlined quantities in (7) denote matrices and vectors in the matrix space. $\underline{\vec{k}}$ and $\underline{\vec{p}}$ are vectors both in this space and in Lorentz space so that, for example, the first term in (7) represents a double sum

$$k^{\mu}_{j} \quad A_{ij} \quad k^{\mu}_{j}$$

both over the matrix indices i, j and over the Lorentz index μ. If we define

$$D = - (\underline{B\vec{p}})^{T} \; \underline{X} \; \underline{B\vec{p}} + (\vec{p}^{T} \underline{\Gamma} \vec{p} - \sigma) \; C \qquad (8)$$

where

$$X = \text{adj } A \qquad (9)$$

$$C = \det A \qquad (10)$$

the result of performing the k - integration in (1) is, apart from a constant factor,

$$I = \int_{0}^{1} \prod_{i} d\alpha_{i} \; \frac{\delta(\Sigma\alpha_{i} - 1) \; C^{N-2\ell-2}}{D^{N-2\ell}} \qquad (11)$$

In fact the expression (8) for D is equivalent to

$$D = CD' \qquad (12)$$

where D' is the result of eliminating k from ψ according to (3), which in the new notation reads

$$\underline{A}\,\vec{k} = \underline{B}\,\vec{p} \qquad (13).$$

Thus we see that the Hadamard equations (3) and (4) applicable to the representation (1) for $I(z)$ are together equivalent to the equations

$$\frac{\partial D}{\partial \alpha_1} = 0 \qquad (14)$$

which are the Hadamard equations for the representation (11).

1.2 Dual Diagrams

The conditions (5) and (6) lead to the dual diagram analysis of Landau and of Taylor[13]. A dual diagram is a vector diagram in which each line is on the mass shell. The E external momenta form a closed polygon in the diagram, expressing the fact that energy-momentum is conserved over all. The squares of their lengths, together with those of the diagonals of the polygon, are the variables z of which I is a function. The inclusion of the internal lines for the graph in the diagram imposes a single constraint on the polygon, so that an equation is obtained connecting the z that is the equation of an analytic manifold in z-space. This manifold is known as the Landau curve. Its equation evidently involves the internal masses m_i.

The condition (5) usually implies a geometrical constraint on the lines in the dual diagram: without it no equation connecting the z would be obtained. For example, in the case of the single loop triangle graph it demands that there be a vanishing linear combination of the lines in the dual diagram that

represent the three internal vectors. Hence they, and therefore the whole diagram, must be drawn in a plane. Unfortunately the geometrical constraints implied by (5) are not always so simple.

The single loop graph is an example of a proper graph: it may be drawn in such a way that its lines are joined wherever they cross and the dual diagram may be drawn using the standard Bow's notation for finding the stresses in rigid frameworks. Such a diagram is characterised by the fact that one line in the Feynman graph corresponds to one line in the dual diagram and the vectors round any loop of the graph all converge at one point in the dual diagram. Improper dual diagrams, corresponding to Feynman graphs which cannot be drawn with all lines joined where they cross, do not have these characteristics. The simplest example is the improper graph of figure 1, whose dual diagram is drawn in figure 2.

The space in which dual diagrams are drawn may conveniently be Euclidean. The coordinates of its vertices in this space are not necessarily real so that, for example, distinct points may be separated by zero distance.

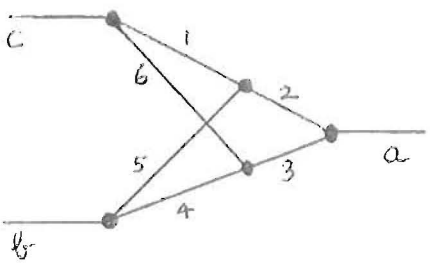

Fig. 1

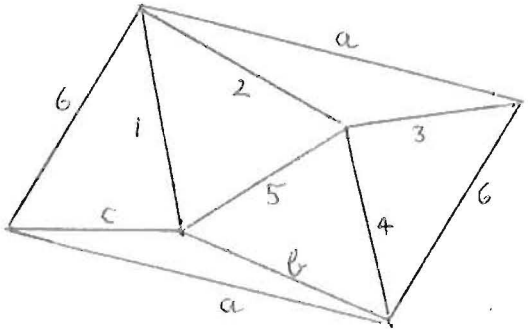

Fig. 2

It is not always the case that dual diagrams are drawn in a space of the same dimensions as that spanned by the external vectors of the graph. However, since the integration over the $\vec{k}$ in (1) is four-dimensional, corresponding to the fact that space has four dimensions, the maximum number of dimensions available for the construction of a dual diagram is four. Hence, for example the leading curve for the sixth order single loop graph does not exist, though it would exist if space were five dimensional. The effect of the dimensionality of space on analyticity properties has been noted before[16].

We examine further the case when the dual diagram is drawn in a space of greater dimensions than that spanned by the external vectors. An example is the

graph of figure 3, whose dual diagram is drawn in figure 4.

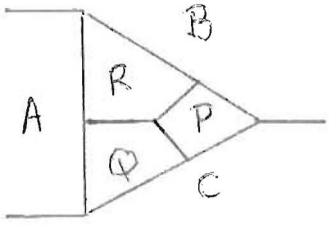

Fig. 3

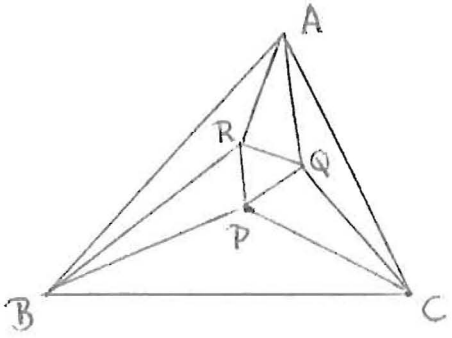

Fig. 4

The dual diagram is over determined in a plane when AB, BC, say, are fixed in advance, but may be drawn in three dimensions with one degree of freedom. The degree of freedom is taken up when condition (5) is applied, and then the length BC is determined.

For a general dual diagram of this type, where the external vectors span a space of less than four dimensions so that their fourth components may be taken as zero, the fourth component of the equations (13) gives a solution with the fourth components of the k not all zero if and only if

$$C = \det \underline{A} = 0 \qquad (15).$$

This equation cannot be satisfied when all the α are real and positive since C is the sum of products of the α[17]. This may also be seen geometrically for proper dual diagrams*: in the real subspace of the complex Euclidean space in which the diagram is drawn one of the vertices of the diagram is furthest away from the real subspace spanned by the external vectors. The vectors converging at that point cannot have a vanishing linear combination with all the coefficients α positive. This result has the important consequence that in the case of propagator graphs the only singularities on the physical sheet are the normal thresholds. Any other propagator graph has a dual diagram which requires more than one dimension for its construction and so does not yield α which are all positive. In the case of a propagator this means the corresponding singularity is not on the physical sheet. This can be seen using the representation (11) and the fact that the expression (8) for D contains the z linearly, the coefficients of each z being a sum of products of the α[17]. Hence if, as for a propagator, there is only one z, D does not vanish for complex z and real positive α. Thus the

* For improper dual diagrams a geometrical proof is not apparent.

hypercontour of integration need never be distorted if we let z tend to the real z-axis. Further, D does not vanish for z real and sufficiently negative, so that we may cross the real axis in the continuation process. This is sufficient to prove the statement; such arguments will be used more elaborately in the next chapter.

1.3 Second-Type Solutions

The dual diagram analysis does not yield all possible solutions of the Landau equations. The extra solutions will be called second-type solutions and correspond to infinite values for some of the components of the internal momenta $\vec{k}$. This does not imply that the resulting singularities of the Feynman integral depend on the range of integration over the $\vec{k}$ being infinite. They would be present also if the range of integration were finite and arise from distortions of the integration hypercontour, consequent on analytic continuation, extending to infinity. In the case of a finite integral there would be additional singularities associated with the boundary of the region of integration. The latter is absent in the infinite integral: the hypercontour is topologically closed.

Second-type solutions fall into two classes: pure second-type and mixed. The presence of the latter may be deduced from that of the former as follows. Consider a graph G that has more than one loop. It may be divided (in a number of ways) into two subgraphs G_1 and G_2. Let the Feynman function for G_1 be f. Then

the Feynman function for G is equal to a multiple integral whose integrand is f multiplied by a propagator for each line that is internal to G but not to G_1. A mixed singularity occurs when a pure second-type singularity of f pinches with the poles of the propagators.

We shew that for a pure second-type singularity the equation of the manifold in z-space is the Gram determinantal relation

$$\det \vec{p}_i . \vec{p}_j = 0 \qquad i, j = 1, 2 \ldots (E-1) \qquad (16)$$

that arises when the dimensions of the space spanned by the external vectors is less than (E-1), or more generally when there exists a subspace of dimension less than (E-1) such that the component of each external vector p perpendicular to this subspace has zero length. The equation does not involve the internal masses m_i, unlike that of a Landau curve derived from a dual diagram.

We shew, then, that when C, defined by equation (10),

is put equal to zero there are many solutions of the equations (14). If the L x L matrix $\underline{A}$ is of rank (L - 1) its adjoint can be written

$$\underline{X} = \underline{K}\,\underline{K}^{T} \tag{17}$$

where the column matrix $\underline{K}$ satisfies

$$\underline{A}\,\underline{K} = 0 \tag{18}$$

Let $\underline{\Lambda}$ be any column matrix and $\vec{\lambda}$ a zero-length vector in Lorentz-space:

$$\vec{\lambda}^{2} = 0 \tag{19}$$

Suppose also

$$\vec{\lambda}.\vec{p} = 0 \tag{20}$$

for each external vector $\vec{p}$ of the graph.

Let $\vec{k}$ be vectors that are linear combinations of the $\vec{p}$ and satisfy the equation

$$\underline{A}\,\vec{\underline{k}} = \underline{B}\,\vec{\underline{p}} - \underline{\Lambda}\,\vec{\lambda} \tag{21}$$

A necessary and sufficient condition for such $\vec{k}$ to exist is that

$$\underline{K}^{T}\,\underline{B}\,\vec{\underline{p}} = \vec{\lambda}\,\underline{K}^{T}\,\underline{\Lambda} \tag{22}$$

Equations (20) and (22) together require there to be a linear combination of the $\vec{p}$ that is equal to a zero-length vector whose scalar product with each $\vec{p}$ vanishes. Thus they lead to the Gram condition (16).

If we denote differentiation with respect to α_i by the subscript i we obtain from (8)

$$D_i = -(\underline{B}\,\vec{p})^T \cdot \underline{X}_i\,\underline{A}\,\vec{k} + (\vec{p}^T \Gamma\, \vec{p} - \sigma)C \qquad (23)$$

Here we have used the condition $C = 0$ and equations (17), (18) and (21), together with the fact that the matrix $\underline{A}$ is symmetric. Now

$$\underline{X}\,\underline{A} = C$$

so that

$$\underline{X}_i\,\underline{A} + \underline{X}\,\underline{A}_i = C_i$$

and hence

$$D_i = C_i\,\psi(p, k, \alpha) \qquad (24)$$

Thus the Hadamard equations $D_i = 0$ are satisfied for $\vec{k}$ chosen as above provided also $\psi = 0$.

If in the above we choose $\vec{\lambda} = 0$ we may dispense with the condition that the solution $\vec{k}$ to (21) be a

linear combination of the $\vec{p}$ and we obtain similar results. Thus the Hadamard equations (14) are solved by applying (5) to any vector diagram such that the (E - 1) vectors $\vec{p}$ that are generally independent fulfil the Gram condition (16) and the single constraint

$$\psi(\vec{p}, \vec{k}, \alpha) = 0 \qquad (25)$$

It is not necessary, however, that (6) be satisfied. This is at first sight paradoxical, since we have said that (5) and (6) are together equivalent to (14). To resolve this we consider the representation (1) and shew that the second-type solutions arise out of solutions of the Landau equations for which the $\vec{k}$ are infinite. In order to make infinity accessible to our analysis it is convenient to introduce homogeneous coordinates

$$\vec{\underline{k}} = \vec{\underline{K}} \zeta^{-1} \qquad (26)$$

so that the hyperplane at infinity is

$$\zeta = 0$$

Define

$$\Phi(\vec{p}, \vec{k}, \zeta, \alpha) = \vec{\underline{K}}^T \underline{A} \vec{\underline{K}} - 2 \vec{\underline{K}}^T \underline{B} \vec{\underline{p}} \zeta + (\vec{\underline{p}}^T \vec{\underline{p}} - \sigma) \zeta^2 \qquad (27)$$

The conditions for an extremum of ψ are

$$\frac{\partial \psi}{\partial \vec{K}} = 0 \quad , \quad \frac{\partial \psi}{\partial \zeta} = 0 \quad , \quad \frac{\partial \psi}{\partial \alpha} = 0 \tag{28}$$

which on $= 0$ give

$$\left.\begin{aligned} \underline{A}\,\vec{\underline{K}} &= 0 \\ \vec{\underline{K}}^{T}\,\underline{B}\,\vec{p} &= 0 \\ \vec{\underline{K}}^{T}\,\underline{A}_{i}\,\vec{\underline{K}} &= 0 \end{aligned}\right) \tag{29}$$

The equations (29) are given a solution in the following way. Choose the α so that $C = 0$. Then there exists a column matrix $\underline{K}$ satisfying (18). Take

$$\vec{\underline{K}} = \underline{K}\vec{\lambda}' \tag{30}$$

where $\vec{\lambda}'$ is a Lorentz vector, chosen such that

$$\vec{\lambda}'(\underline{K}^{T}\,\underline{B}\,\vec{p}) = 0 \tag{31}$$

to satisfy the second equation in (29) and such that

$$\lambda'^{2} = 0 \tag{32}$$

to satisfy the third equation in (29).

The above solution exists for all $\vec{p}$ and we can therefore deduce that it does not correspond to a singularity of the Feynman integral. The reason for this is as follows. The general idea behind the Hadamard lemma is that a singularity of the multiple integral arises for z such that the hypercontour of integration is pinched by the singularities of the integrand. The Landau equations are the necessary

conditions for such a pinch to occur. But if they are satisfied for all z and if the integral is known to exist for some value z_0 of z they are not sufficient to produce a singularity. This is because, since the integral is defined at z_0, the hypercontour is not trapped at z_0 and so as one continues analytically from z_0 it does not become trapped unless there is a change in the topological character of the intersection of the hypercontour with the manifold of singularity of the integrand.

We therefore seek the condition for the equations (28) to be satisfied also at a point in the integration space adjacent to one of the solutions already found. Let this point be

$$\vec{K}+\delta\vec{K},\quad \delta\zeta,\quad \alpha+\delta\alpha$$

Then (28) requires

$$\underline{A}\,\delta\vec{K} = \underline{B}\vec{p}\,\delta\zeta - \delta\underline{A}\,\underline{K}\vec{\lambda}'$$

$$-\delta\vec{K}^T\underline{B}\vec{p} + (\vec{p}^T\underline{\Gamma}\vec{p} - \sigma)\delta\zeta - \lambda'\vec{K}^T\delta\underline{B}\vec{p} = 0 \qquad (33)$$

$$\vec{\lambda}'\underline{K}^T\underline{A}_i\,\delta\vec{K} - \vec{\lambda}'\underline{K}^T\underline{B}_i\vec{p}\,\delta\zeta = 0$$

The first of these equations is equivalent to (21) with $\vec{k}$ set equal to $\delta\vec{K}/\delta\zeta$. If $\vec{\lambda}'$ is made to satisfy (20) rather than the weaker condition (31) the second

equation in (33) is equivalent to (25). The third equation in (33) is most simply satisfied by taking $\vec{\lambda}' = 0$, or otherwise by making $\delta\vec{K}$ a linear combination of the $\vec{p}$.

We have thus reproduced the conditions for construction of the vector diagram associated with equation (25). The internal lines of this vector diagram are not on the mass shell, but since they do not in fact represent the internal momenta for the Feynman graph, only increments thereof, this does not imply that for second-type singularities the internal vectors are not on the mass shell.

2. Physical Sheet Properties

2.1 Singularities and Cuts

We have seen how, in principle, we may find the equation of the Landau curves in z - space on which the singularities for a given graph may lie. It is more difficult to decide which parts of the Landau curves are actually singular on the physical sheet.

Let us consider how it is possible for one part of a Landau curve to be singular and another not. The Landau curve, S, is the collection of points in z - space for which the manifold D = 0 in α - space degenerates and is locally conelike. S is actually singular if the hypercontour A is pinched between the two halves of D so that it cannot be distorted away from D.

Suppose we are at a point of S which is singular and that we move away from it, remaining on S. A was originally pinched between the two parts of D and as we move D remains locally conelike. The vertex of the cone moves, dragging A with it, so that we are still at a singular point. There are two ways that

this situation can change. The first is that the vertex of the cone falls off on edge of A. Such an edge is in a subspace in which at least one α is zero. Thus the critical points are those in which S meets a lower-order Landau curve, S', in such a way that the two curves give common values of the α at their intersection. This we call an effective intersection. It is easy to shew that S and S' touch at an effective intersection.

The intersections of S with lower-order curves do not form a set of sufficient dimensions to divide S into singular and non-singular sections: a path on S may always be chosen to connect any two points of S and not pass through any effective intersection. However, such a path may cross a cut and so leave the physical sheet. Since our concern is with physics we must in fact not cross cuts but go around the singularities generating them. Alternatively, if we cross a cut we must ensure that we cross back again onto the physical sheet. (We may think of this procedure as being equivalent to temporarily pushing back the cut, whose precise location is in any case arbitrary - except for its branch point). If both these alternatives fail we are forced to go through the effective intersection with a singular lower-order curve and so may change from

singularity to non-singularity.

Thus we conclude that cuts attached to lower-order singularities may divide singular parts of S from non-singular parts. Effective intersections with lower-order curves that are not themselves singular at the intersection need not concern us since these have no cuts attached to them.

The second mechanism by which the singularity behaviour along a path on S can change occurs at a"double pinch". This is best illustrated for the case of a one-dimensional integral. A pair of zeros of D that pinches the integration contour meets a third zero of D. One of the zeros forming the pinch can then change its mate and pair with the new zero. If the new zero is on the same side of the contour this process "dissolves" the pinch, as illustrated in figure 5. The Landau surface

Fig. 5

requires only that a pair of zeros be coincident; thus, if two pinching zeros meet a third zero, we have a singular point of the Landau curve (in the geometrical sense).

We generalise this to a multidimensional integral. We recall that [17] D may be written in the form

$$D = \sum_k f_k z_k + K \qquad (34)$$

where the f_k are in fact sums of products of the α. Hence on the Landau curve

$$0 = d\frac{\partial D}{\partial \alpha_i} = \sum_k \frac{\partial f_k}{\partial \alpha_i} dz_k + \sum_j \frac{\partial^2 D}{\partial \alpha_i \partial \alpha_j} d\alpha_j \qquad (35)$$

At a cusp of the Landau curve $dz_k = 0$, so that

$$\sum_j \frac{\partial^2 D}{\partial \alpha_i \partial \alpha_j} d\alpha_j = 0 \qquad (36)$$

Thus the N x N matrix $\partial^2 D / \partial \alpha_i \partial \alpha_j$, which is normally of rank (N - 1) at a point of the Landau curve, becomes of rank (N - 2). This implies that the cone on the manifold D has degenerated and the intersection of D with the hypercontour involves more points than is necessary for the pinch.

2.2 The Vertex Function

The singularities of the single loop triangle graph were investigated by Källén and Wightman[9] in order to obtain guidance as to the nature of the holomorphy envelope, implied by the axioms, for the three-point function. Calculation of the holomorphy envelope would have been an impossible task without this guidance. The perturbation theory singularities only give part of the boundary of the holomorphy envelope; this is probably because unitarity has not been fully incorporated in the general approach.

Källén and Wightman obtained the information they required by explicit integration. However, the result of the integrations is unpleasant and we shall here use our more general procedure to obtain the results which we shall particularly need later in considering production processes. Our methods were inspired by the treatment of the single loop scattering graph given by Tarski[18] and are a refinement of his techniques.

For the vertex function there are three scalar

invariants, the squares of the masses of the external particles. We shall allow two of them, z_1 and z_2, to vary and fix the third at a value $z_3 = M^2$ consistent with stability. The leading Landau curve for the single loop graph is particularly simple in form, its section in the real (z_1, z_2) plane being an ellipse (figure 6). It touches the lines N which are the

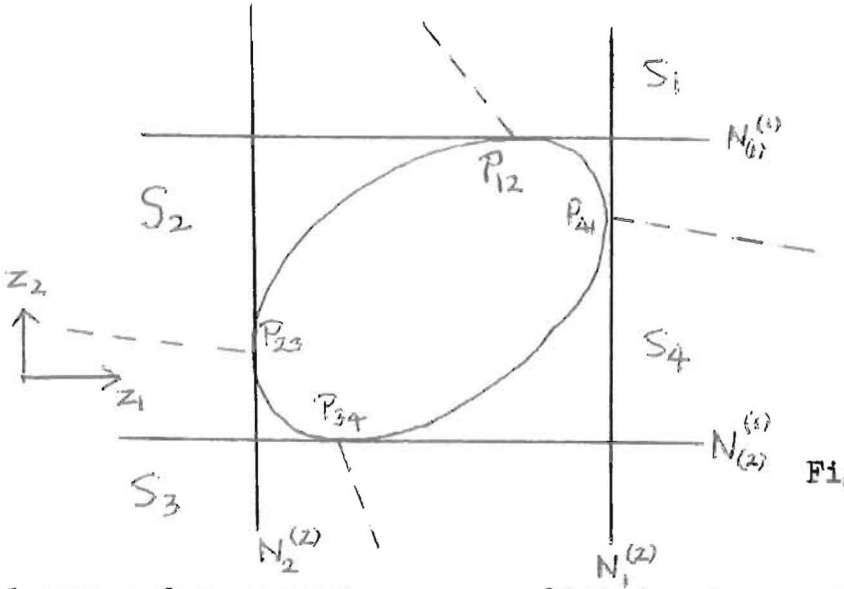

Fig. 6

lower-order curves corresponding to the contractions of the Feynman graph into propagators (figure 7). Of these, $N_1^{(1)}$ and $N_1^{(2)}$ are the normal

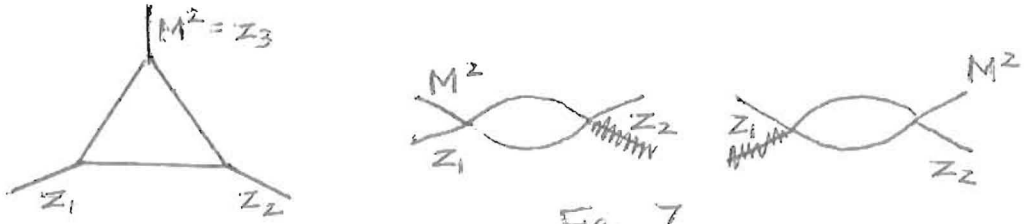

Fig. 7

thresholds and so have cuts attached to them, running by convention along the positive real z_1, z_2 axes and extending to infinity, while $N_2^{(1)}$ and $N_2^{(2)}$ are not singular on the physical sheet. The contacts P of the ellipse with the lower-order curves N are effective intersections.

In addition to the real ellipse the Landau curve has complex portions. Consider its intersections with the real searchline

$$z_1 = \lambda z_2 + \mu \qquad \lambda, \mu \text{ real}$$

and allow λ, μ to vary. The intersections are either real points or pairs of complex conjugate points and the transition from one case to the other takes place when the searchline touches the ellipse. Thus complex conjugate surfaces of S sprout out from the real section and extend to infinity.

For a searchline with $\lambda>0$, Im z_1, and Im z_2 are the same sign; if it is less than 0 they are opposite in sign. Thus the sections S_2 and S_4 of S sprouting from the arcs $P_{12}\ P_{23}$ and $P_{34}\ P_{41}$ of the ellipse (of positive slope) have on them only points for which Im z_1, Im z_2 are of the same sign, while the sections S_1 and S_3 joined to $P_{41}\ P_{12}$ and $P_{23}\ P_{34}$ (of negative slope) give opposite signs. The divisions between these sections (indicated schematically in figure 6 by broken lines) correspond to intersections of S with searchlines of the form z_1 = real and z_2 = real.

The searchline method is applicable to any real algebraic curve. This is useful since the form of the Landau curve in the four-dimensional complex (z_1, z_2) - space may usually be adequately represented by drawing its real section.

We have said that the coefficients of z_1 and z_2 in the Feynman denominator D are just sums of products of the integration variables α. D does not vanish for sufficiently negative Re z_1, Re z_2 and positive α. In this region R of z-space the value on the physical

sheet of the Feynman integral is obtained by integrating over the undistorted hypercontour on which the α are real and in the range (0, 1). Analytic continuation out of this region is made by suitable distortion of the hypercontour. We can also see that D does not vanish for real, positive α when Im z_1, Im z_2 have the same sign. The immediate proof of the existence of so large a region of analyticity is a simplifying circumstance which unfortunately does not generalise.

Since part of S_3 lies in R the whole of that section is not singular. Nor are S_4 and S_2 because on them Im z_1, Im z_2 have the same sign, but in any case there are no cuts dividing them from S_3. However, to get from S_4 to S_1 it is necessary to cross the cut attached to $N_1^{(2)}$, while to reach it from S_2 the cut attached to $N_1^{(1)}$ must be crossed. Consequently S_1 can be singular and in fact it is. This is because the arc $P_{12}\ P_{41}$ lies outside the cuts and corresponds to positive values of the α, which may be seen from the fact that on $N_1^{(1)}$ and $N_1^{(2)}$ two of the α are positive and one zero. The argument of the end of

section 1.2 implies that the arc, and therefore the whole of S_1, is singular, a fact that will be seen in chapter 3 to have unfortunate consequences for production processes.

The triangle graph also has a second-type singularity. Its presence was first pointed out by Cutkosky[19], who finds that the discontinuity across the cut attached to the leading singularity just discussed is

$$\frac{1}{4\sqrt{\lambda(z_1, z_2, z_3)}} \tag{37}$$

where

$$\lambda(z_1, z_2, z_3) = z_1^2 + z_2^2 + z_3^2 - 2z_2z_3 - 2z_3z_1 - 2z_1z_2 \tag{38}$$

This expression has a singularity given by

$$\lambda(z_1, z_2, z_3) = 0 \tag{39}$$

which is just the Gram determinantal condition (16). Since (37) is the difference between the values of the original Feynman function on two of its Riemann sheets, the original function possesses this singularity

also. It does not appear on the physical sheet: this is a general property of pure second-type singularities that will be demonstrated in section 2.5.

2.3 The General Scattering Graph

In a scattering process, involving four particles of fixed mass, there are three scalar invariants s, t, u. These are linearly related: their sum is equal to the sum of the squares of the masses of the external particles. For an improper graph all three may appear in the denominator function D, so that in general, on elimination of u, say,

$$D = (f - h)s + (g - h)t + K$$

where now f, g, h are sums of products of the α. Thus it is no longer immediate that there exists a tube R of z-space (z_1, z_2 being any pair of s, t, u) in which D does not vanish for real positive α. Symanzik[17], however, has shewn that such a tube does exist provided the masses of the external particles are not too large compared with those of the internal particles*.

Basically the same techniques as described for the

---

* D does vanish when all the α corresponding to the lines around any loop of the graph are zero. This leads to difficulties, but not serious ones.

single-loop. vertex graph may be applied to the general scattering graph. Naturally the latter is considerably more complicated, but one property which generalises is that when the Symanzik region R exists a point on S and its complex conjugate (also on S) are either both singular or non-singular on the physical sheet. This is because, as we continue from a real point in R to some point (z_1, z_2) along some route in z-space, we end up with a certain configuration in α-space of the hypercontour A and the manifold D of zeros of the denominator. If we continue instead to (z_1, z_2) along the complex conjugate route we merely end up with the conjugate configuration. (This may otherwise be seen by the reflection principle of complex variable theory). It must be shewn that this prescription gives the value of the Feynman amplitude on the physical sheet; this has been discussed by Polkinghorne and Screaton[20].

An improper scattering graph has normal threshold cuts corresponding to each of the three invariants s, t, u. However at any point in the real plane at most two of these cuts overlap. The corresponding

invariants are the most appropriate for discussing behaviour at the point. The reality property implies that there are not more than two distinct limits on the real section C of S at the point: that in which the imaginary parts of the two variables take the same sign and that in which they have opposite sign. On C the limit defined by approach in the same sense as the attached complex part of S is called the appropriate limit. At points where there is only one cut both limits must coincide, since the way in which the limit is taken for the variables not having the cut is immaterial.

Most of the work[3, 4, 22] on scattering graphs has been devoted to attempts to prove a conjecture of Mandelstam that the domain of holomorphy for the scattering amplitude is the topological product of the complex s, t, u planes with cuts along their real axes starting at the normal thresholds. An induction procedure on the order of the graph is used: it is supposed that there are no anomolous thresholds (singularities arising from vertex graphs) and that the Mandelstam conjecture is valid for each of the

contracted graphs obtained from that under consideration.

Only the most important points in the work are mentioned here. Further details may be found in references 3, 4, 22. The basic method is to try and divide the Landau curve into a number of sections, each of which is either wholly singular or non-singular. If a section intersects the manifold on which s, t, or u corresponds to forward scattering the existence of a forward scattering single-variable dispersion relation suffices to prove the section non-singular for the case of equal external masses. Other cases are treated by analytically continuing from this one by varying the external masses: they may even be varied beyond the limit for the appearance of an anomalous threshold[4].

An important property required for the discussion of the division of S into sections is that the normal threshold curves, which are inevitably singular, can only have effective intersection with the leading curve at infinity. This we may shew by noting that when S has effective intersection with a normal threshold it necessarily also has effective intersection

at the same point with a curve corresponding to a vertex graph. But both these lower-order curves are sets of parallel straight lines, so this can only happen at infinity.

The primitive sections into which S is divided by the normal threshold cuts are linked together to form a section that intersects a forward scattering manifold. This process is illustrated by figure 8.

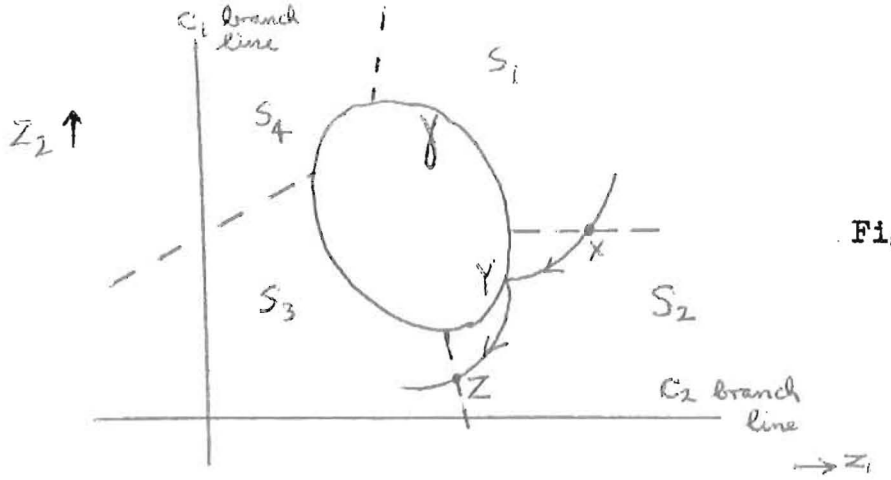

Fig. 8

Here γ is a loop which is part of the real section of S, lying in the region where two cuts C_1 and C_2 overlap. From it sprouts a complex part of S which is divided by C_1 and C_2 into four primitive sections. We link S_1 to S_3 by a path lying in S.

This can be done by following the type of path P sketched in figure 8. At X we cross C_1. At Y we cross γ and move on to the complex conjugate half of S_2. In doing so we recross C_1 and also cross C_2. At Z we recross C_2. Between X and Z we have left the physical sheet and are in a neighbouring unphysical sheet, but at Z we re-enter the physical sheet and so arrive at S_3. on the physical sheet. The projections of P on the complex z_1 and z_2 planes are shewn in figure 9.

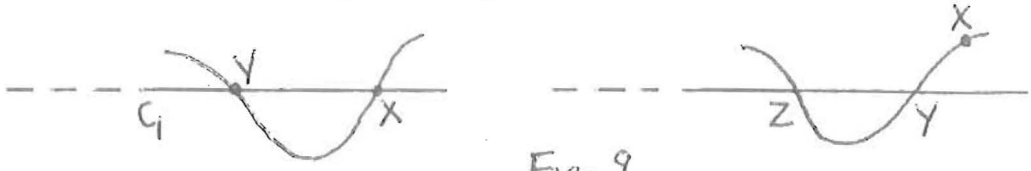

Fig. 9

No change in behaviour on P will have occurred unless we have encountered a lower-order singularity between X and Z. The induction hypothesis must be invoked to demonstrate that this can be avoided.

The procedure just outlined is not sufficient to prove the Mandelstam conjecture. The reason for this will be shewn by an example in the next section.

2.4 The Acnode Graph[6]

Consider the graph of figure 10, whose dual diagram is drawn in figure 11. We take each mass equal to unity except for the two external

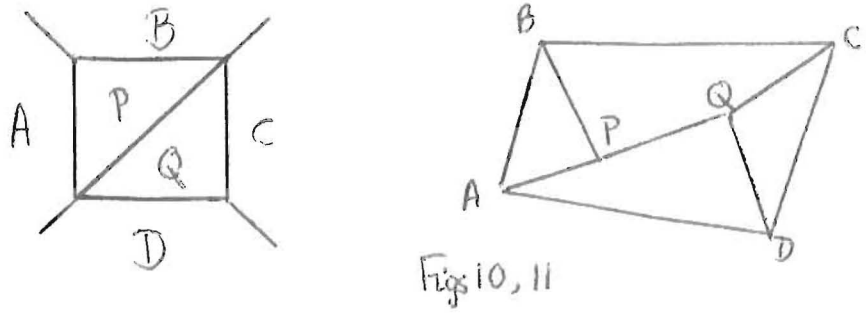

Figs 10, 11

masses BC and AD which we take to be M. We choose a solution having $\alpha_{AP} = \alpha_{CQ}$ and $\alpha_{BP} = \alpha_{DQ}$ and so obtain parametrically the equation of part of the Landau curve:

$$s = 5 + 4\cos\phi + 2\left(2 - \tfrac{1}{2}M^2 + \cos\theta + \cos\phi\right)\sin\phi/\sin\theta \qquad (40)$$

$$t = \theta \leftrightarrow \phi$$

where $\theta + \phi = \pi$. θ and ϕ are in fact the angles between PQ and AP, BP produced. On this part of the curve they are also equal to the angles between PQ and CQ, DQ produced. It can be seen that when θ or ϕ tends to zero, the curve is asymptotic to the normal thresholds $s = 9$ or $t = 9$.

The Feynman parameters are given by

$$\frac{\alpha_{AP}}{\sin\phi} = \frac{\alpha_{BP}}{\sin\theta} = \frac{2\alpha_{PQ}}{\sqrt{3}} = \frac{\alpha_{CQ}}{\sin\phi} = \frac{\alpha_{DQ}}{\sin\theta} \qquad (41)$$

All the α are real and positive when

$$0 < \theta < \pi/3 \quad , \quad 0 < \phi < \pi/3 \qquad (42)$$

The part of the real curve for which θ and ϕ are in the range (42) is drawn in figure 12 for various values of M^2. For $M^2 < 4 + 2\sqrt{2} = 6{\cdot}828$ it has the form shewn in figure 12 (a). To obtain the form as M^2 increases past this value we take

$$\theta = \pi/6 + i\eta \qquad \phi = \pi/6 - i\eta \qquad (43)$$

When $4 + 2\sqrt{2} < M^2 < 4 + 5\sqrt{3}$ there are real non-zero values of η such that

$$\mathrm{Ims} = \mathrm{Imt} = 0 \qquad (44)$$

Thus at $M^2 = 4 + 2\sqrt{2}$ coincident acnodes appear on the line $s = t$, and as M^2 increases further they separate,

giving the arc and two acnodes shewn in figure 12 (b). At the value $M^2 = 4 + 5/\sqrt{3} = 6{\cdot}887$ one of the acnodes

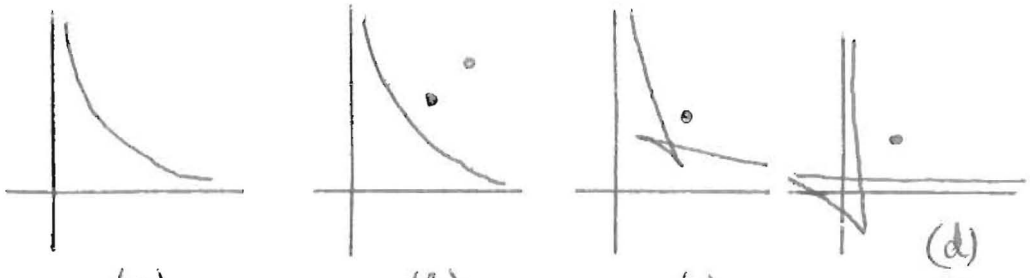

Fig. 12

lies on the curve. Above this value of M^2, this acnode has changed into a crunode and there are two ceratoid cusps on the curve as in figure 12 (c). The positions of the cusps can be found from

$$ds/d\theta = dt/d\theta = 0 \qquad (45)$$

For $M^2 < 4 + 5/\sqrt{3}$, the equations (45) have a pair of solutions that correspond to complex s, t. They are complex cusps and play an important part in our discussion.

As M^2 increases further, the two cusps cross the normal thresholds; and for $7 > M^2 > 4\sqrt{3} = 6{\cdot}928$ part of the arc lies outside the crossed cuts (figure 12 (d)).

Above $M^2 = 7$ there are anomalous thresholds and the character of the curve changes in a manner we need not discuss here.

The curves drawn in figure 12 correspond to most of the masses being equal. No radical change in their character can be introduced by breaking the equalities because this part of the Landau curve can have no horizontal or vertical tangents. Because of the explicit form of D in the present case such tangents can only be the straight line Landau curves corresponding to the vertex graphs obtained from figure 10 by contracting one of the internal lines. These do not lie above the normal thresholds.

The complex part of the Landau curve, attached to the real arc in figure 12, is complicated in nature. Consider intersections of the Landau curve with the searchlines

$$s + t = \mu \qquad (46)$$

where μ is a real parameter. The paths traced out in the complex s (or t) plane as μ is varied are

shewn in figure 13 for the case of figure 12 (b).

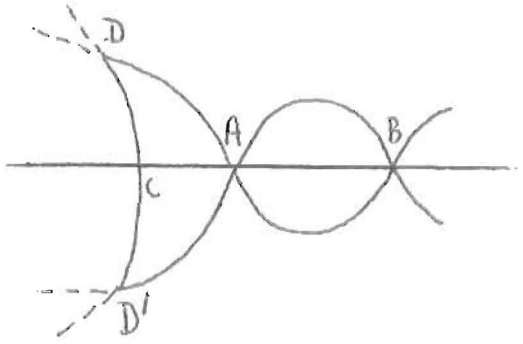

Fig. 13

The acnodes are labelled A, B, the midpoint of the real arc is denoted C, and D, D^1 are complex cusps. The parts of the paths drawn in solid line correspond to real η and those in broken line to complex η .

When the Landau curve has the form shewn in figure 12 (a) the real arc is singular in the inappropriate limit but not in the appropriate limit. If now M^2 is increased the Landau surface changes continuously and it is possible for a real or complex part to become singular on the physical sheet only if that part grows from zero size. As M^2 increases past the value $4 + 2\sqrt{2}$ the two acnodes appear, at first coincident, and so the complex piece T of Landau curve between them may be singular. At first sight one might hope that one could use the type of argument

associated with figures 8 and 9 to shew that this is not so, but this argument depended crucially on the two portions of complex surface joined tothe real curve being connected by a path through the real curve such that the α changed continuously on the path. Here the arcs BAD and BAD^1 share common values of the α neither at A nor at B.

To determine whether T is in fact singular, we increase M^2 further until $M^2 > 4\sqrt{3}$, when the situation of figure 12 (d) has been reached. During this variation of M^2, T remains finite in size and does not cross any cuts. The situation of figure 12 (d) has part of the real Landau curve outside both normal threshold cuts, and on this part of the curve the α are positive. Hence this part is singular from any limit and therefore also the piece of complex surface attached to it. This is the piece that T has grown into as M^2 was increased. Hence T is singular as soon as it appears.

This would not be possible were it not for the presence of the complex cusps D, D^1. In the case

associated with figures 8 and 9 to shew that this is not so, but this argument depended crucially on the two portions of complex surface joined tothe real curve being connected by a path through the real curve such that the α changed continuously on the path. Here the arcs BAD and BAD^1 share common values of the α neither at A nor at B.

To determine whether T is in fact singular, we increase M^2 further until $M^2 > 4\sqrt{3}$, when the situation of figure 12 (d) has been reached. During this variation of M^2, T remains finite in size and does not cross any cuts. The situation of figure 12 (d) has part of the real Landau curve outside both normal threshold cuts, and on this part of the curve the α are positive. Hence this part is singular from any limit and therefore also the piece of complex surface attached to it. This is the piece that T has grown into as M^2 was increased. Hence T is singular as soon as it appears.

This would not be possible were it not for the presence of the complex cusps D, D^1. In the case

shewn in figure 12 (b) the real arc is not singular in the inappropriate limit. Hence the part of complex surface, represented by AD (or AD') in figure 13, attached to it and lying in the neighbouring unphysical sheet is also nonsingular. We can follow a path on this surface, passing through the complex cusp D to reach the acnode A. We can then continue on this path back into the physical sheet on to T and would conclude that T is nonsingular were it not for the second mechanism, involving passing through a cusp, by which the singularity behaviour along a path on the Landau curve can change. This was discussed in section 2.1. If we choose a path that does not pass through the cusp it can be verified* that its projection on the complex s or t plane necessarily goes round the cusp in one or other variable but not in both. Hence such a path goes through the cut attached to the singular part of the Landau curve in the neighbourhood of the cusp and ends up on the wrong Riemann sheet.

*We are grateful to Mr. P. Swinnerton-Dyer and Mr. C. Paradine who performed computations on EDSAC II in connection with this problem.

2.5 Second-Type Singularities

The analysis of section 2.3 can be used to shew that, at least for the three point and four point functions, the pure second type curve is not singular on the physical sheet.

For definiteness, consider the four-point function. The existence of a forward scattering single-variable dispersion relation shews that not all the second-type curve C is singular on the physical sheet. Since we know its explicit equation we know that the curve C has neither acnodes nor cusps. It cannot have effective intersection with normal or anomalous threshold curves since these are straight lines whose position depends on the internal masses and so they cannot in general touch C whose equation (16) is independent of these masses. There remains the possibility that C has effective intersection with leading curves for four point graphs. However, we can assert that these curves are never singular at these intersections. This is because C is the curve to which the invariants z would be confin ed if Lorentz space were two dimensional, and if space

2.5 Second-Type Singularities

The analysis of section 2.3 can be used to shew that, at least for the three point and four point functions, the pure second type curve is not singular on the physical sheet.

For definiteness, consider the four-point function. The existence of a forward scattering single-variable dispersion relation shews that not all the second-type curve C is singular on the physical sheet. Since we know its explicit equation we know that the curve C has neither acnodes nor cusps. It cannot have effective intersection with normal or anomalous threshold curves since these are straight lines whose position depends on the internal masses and so they cannot in general touch C whose equation (16) is independent of these masses. There remains the possibility that C has effective intersection with leading curves for four point graphs. However, we can assert that these curves are never singular at these intersections. This is because C is the curve to which the invariants z would be confin ed if Lorentz space were two dimensional, and if space

were two dimensional it would not be possible to draw dual diagrams for the leading curve of a scattering graph.

A corrollary of this argument is that starting from a non-singular point of C and moving on C one cannot enter a sheet on which C is singular. This is of significance in connection with analytic properties of partial wave amplitudes since C is the boundary of the region of integration when the partial wave projection is made.

No discussion has been given of the physical sheet properties of mixed second-type singularities. Acnodes and cusps may be expected to occur.

3. Production Processes

3.1 Kinematics

An important difference between scattering and production processes is that for the latter more scalar variables are required to specify the configuration of 4-momenta. For scattering there are only two independent variables, but when $E > 4$ external particles are involved $(3E - 10)$ variables are required. So even the simplest production process, $E = 5$, requires five variables. It will suffice to consider this case here.

Let the 4-momenta of the two incoming particles be p_1, p_2 and of the three outgoing particles $-p_3$, $-p_4$, $-p_5$, so that $\Sigma p = 0$. There are ten scalar products of the form

$$w_{ij} = p_i \, p_j \qquad i \neq j \tag{47}$$

There are several ways in which five of these may be chosen as the independent variables: call them v_{ij}. The remaining five redundant variables, r_{ij}, may then

immediately be expressed as linear combinations of the v_{ij} by use of the identities

$$\begin{aligned} p_i(p_i + p_j + p_k + p_l + p_m) &= 0 \\ (p_i + p_j + p_k + p_l)^2 &= p_m^2 \\ (p_i + p_j + p_k)^2 &= (p_l + p_m)^2 \end{aligned} \tag{48}$$

The result is

$$r_{ij} = \lambda_{ij}^{kl} v_{kl} + \beta_{ij} \tag{49}$$

where λ_{ij}^{kl} is either ± 1 or zero and β_{ij} is composed of squares of the masses of the particles.

Physically, the quantities w_{12}, w_{34}, w_{45}, w_{35} represent energies and the others momentum transfers. The range of physical values which a given w_{ij} may take depends in a very complicated way on the values assigned to the others.

3.2 Complex Singularities

Our results for the vertex function, which was treated in section 2.2, may be used to shew very simply that production processes have complex singularities as functions of two v_{ij} with the remaining three fixed. This is because, however the variables v_{ij} are chosen, there is always a graph of the type drawn in figure 14. Here each of

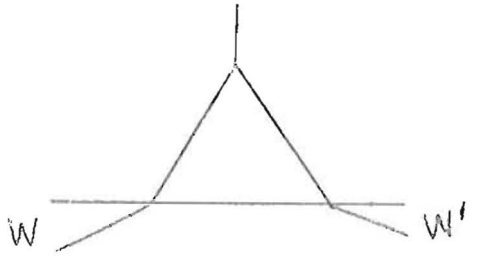

Fig. 14

the scalar products W, W^1 is either one of the two variables v_{ij} or is one of the redundant variables that varies with the latter by virtue of equation (49). Hence figure 14 is just a single-loop vertex graph with two variable masses, which we already know to have complex singularities.

It takes rather more to rule out the possibility of cutplane analyticity when four of the v_{ij} are fixed

at physical values and only one is allowed to vary. We shall call this one V. Consider a graph as in figure 14 where now W varies with V, being either V itself or a redundant variable depending on V through (49), and W^1 is fixed and represents a physical energy. This means that W^1 has a value greater than that for the corresponding normal threshold when W^1 is regarded as variable. Hence the singularities in the complex W-plane for the graph of figure 14 are obtained by considering intersections of the W-W^1 Landau curve with a straight line (A) in figure 15.

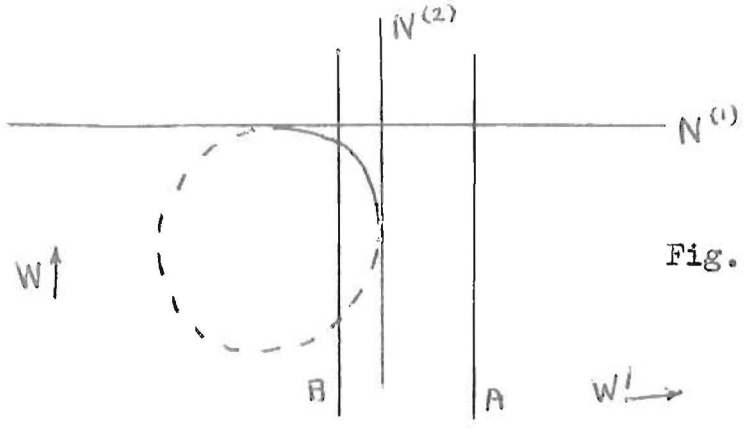

Fig. 15

We recall from Section 2.2 that the Landau curve is an ellipse, and that in the real plane only the arc drawn in solid line is singular. Hence the line (B) has one singular intersection with the Landau curve and one non-singular. If we move (B) towards

the right, these two intersections come together when (B) coincides with the normal threshold $N^{(2)}$ and thereafter separate, moving into opposite halves of the W-plane. In fact we must prevent (B) coinciding with $N^{(2)}$ by giving W^1 a small imaginary part. Then no cuts have been crossed, so that when (B) has come into coincidence with (A) one intersection is still singular and the other not. We decide which is which by considering the Feynman prescription that the physical value of the Feynman amplitude is obtained by giving each internal mass a small negative imaginary part and integrating over an undistorted hypercontour in α-space. This also determines the sign of the imaginary part given to W^1 to avoid the normal threshold $N^{(2)}$. The result is that the singularity lies in the opposite half-plane from that in which the approach is made to the physical limit on the real axis, this being in $\mathrm{Im}W>0$. Hence if $W = +V + \text{const}$, the complex singularity lies in the lower half of the complex V-plane, while if $W = -V + \text{const}$. it lies in the upper half.

There is another simple type of breakdown of analyticity, which is concerned with the normal threshold

graphs, figure 16

Fig. 16

These produce a cut in the W-plane and the physical limit is to be taken on to the real axis from the upper half plane. Consider the contribution to the amplitude from two such graphs, with corresponding variables W, W^1. Suppose that W = +V + const. and W^1 = -V + const. and also that W, W^1 represent energies when they take physical values. Then in the V-plane the two corresponding cuts overlap and the physical region lies completely within the part of the real axis on which they overlap (figure 17)

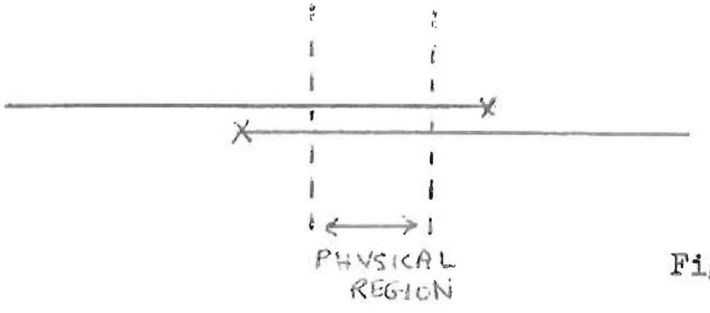

Fig. 17

Further, the physical limit is to be taken between the two cuts, so that on the face of it the physical

value of the amplitude is not the boundary of an analytic function at all. However, this is not so because we may distort the cuts to obtain at least some region of analyticity (figure 18).

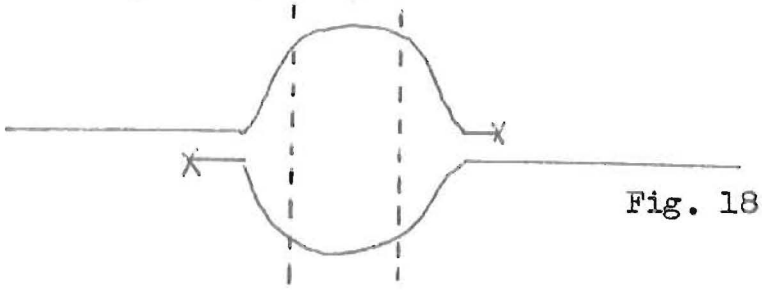

Fig. 18

One might hope that one can in fact swing one cut round through 2π so that the figure is again as in figure 17 but now the physical limit is taken from, say, the lower half plane. But one can see that this is certainly of no avail when there are other normal thresholds corresponding to both W, W^1 in the physical regions. Even when there are not, new complex singularities are likely to be exposed when the cut is swung round. For example, the graph of figure 19 can be seen, from its dual diagram

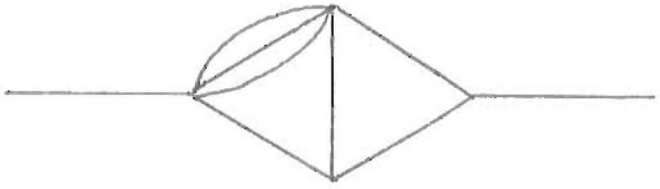

Fig. 19

to have complex singularities on unphysical sheets. It is thought that it has them on that unphysical sheet which is exposed by the swinging round of the cut.

It is a matter of simple but very tedious enumeration to shew that, whatever choice of v_{ij} is made from the w_{ij} and whichever of them is chosen as the variable V, one or other or both of the types of breakdown of analyticity described above is encountered. Further, when the first type occurs there are complex singularities in both half planes. These singularities are branch points and so have cuts attached to them. Thus there is no possibility of a useful dispersion relation when four scalar products are fixed and one varies. We have not entirely ruled out the possibility of a dispersion relation in terms of other "peculiar" variables, but they could not be too peculiar for it to be of any practical value.

3.3 A Particular Process

At the suggestion of Chew and Low[23], much attention has been given to the production process $\pi + N \rightarrow N + \pi + \pi$. Here extrapolation from experimental data is made to the single pion pole in the nucleon-nucleon momentum transfer. It is supposed that the πN interaction is peripheral, so that the main contribution comes from the diagram of figure 20, and that therefore the extrapolation gives

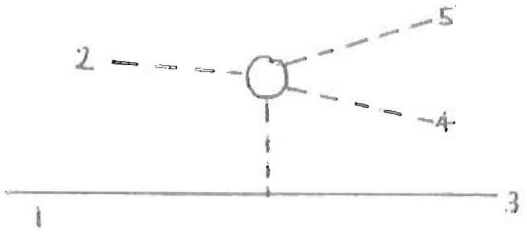

Fig.20

information about the π-π interaction.

For this procedure to be valid it is not necessary that there be a dispersion relation, but that there be sufficient analyticity for there to be no "spurious" singularities near the pole to which extrapolation is

made. In fact, however, the complex singularities considered in the last section do appear near the pole.

With the particles labelled as in figure 20 the basic set v_{12}, v_{45}, v_{24}, v_{34}, $v_{13} \equiv V$ of scalar products is used. The Feynman graph of interest for our purposes is the triangle graph of figure 21. For this graph W^1 and W are respectively the fixed energy v_{34} and the

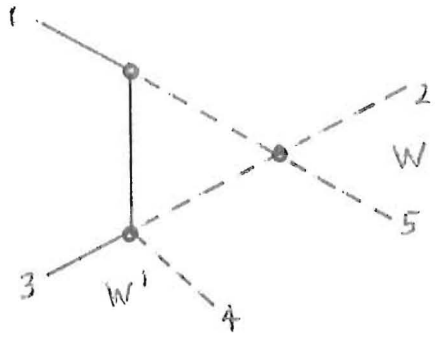

Fig. 21

redundant variable

$$r_{25} = V - v_{24} - v_{45} + 3\mu^2$$

where μ is the pion mass. A simple calculation shews that the complex singularity occurs at

$$V = -\mu^2 + v_{24} + v_{45} - \frac{\mu^3}{M} z - 2i\mu^2 \sqrt{(z^2-1)(1-\mu^2/4M^2)}$$

If one inserts into this formula some typical values encountered in experiments:

$$v_{12} = 144\mu^2 \qquad v_{45} = 12\mu^2 \qquad v_{34} = 61\mu^2$$
$$v_{24} = -10.2\mu^2$$

one finds that the singularity occurs almost exactly at

$$V = (1-i)\mu^2$$

In fact this is even not the set of values of the fixed v which brings the singularity nearest to the pole at $V = \mu^2$. To find this set of values would require an involved calculation, because one has to check that it is a physical set. This is best done using the centre-of-mass system for the process; one has to check that the angles between the outgoing 3-momenta and between the plane of the outgoing particles and the line of the ingoing particles are physical.

3.4 Experimental Predictions

It is our object here to discuss whether the Landau singularities can ever be "noticed" experimentally. The hope is that under favourable kinematic circumstances they may appreciably influence the shape of a cross-section curve. This may be expected to happen when they are infinities rather than mere branch points and they approach close to the physical region. Only the simplest graphs produce singularities that are infinite[20] and we here confine ourselves to a discussion of the simple triangle graphs, which are in fact the only graphs with three vertices that do produce infinities.

Rather than cope with the complicated generalities of the structure of the physical manifold and of the various singularity manifolds for different kinds of graphs, let us turn directly to what is a particularly simple class of graphs. Consider the production reaction

$$k_1 + k_2 \to q + (K_1 + K_2 + \ldots.)$$

where each letter represents a particle and also its

3.4 Experimental Predictions

It is our object here to discuss whether the Landau singularities can ever be "noticed" experimentally. The hope is that under favourable kinematic circumstances they may appreciably influence the shape of a cross-section curve. This may be expected to happen when they are infinities rather than mere branch points and they approach close to the physical region. Only the simplest graphs produce singularities that are infinite[20] and we here confine ourselves to a discussion of the simple triangle graphs, which are in fact the only graphs with three vertices that do produce infinities.

Rather than cope with the complicated generalities of the structure of the physical manifold and of the various singularity manifolds for different kinds of graphs, let us turn directly to what is a particularly simple class of graphs. Consider the production reaction

$$k_1 + k_2 \to q + (K_1 + K_2 + \ldots.)$$

where each letter represents a particle and also its

4-momentum. In particular we shall denote by m the mass of the particle q. We now restrict ourselves to triangle graphs (figure 22) in which the colliding particles k_1, k_2 join at one vertex, the single particle q emerges from a second

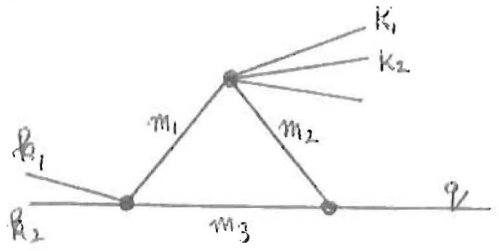

Fig.22

vertex, and the remaining particles K_1, K_2.... all join at the third vertex. Aside from spins, the amplitude for such a graph depends on only two independent variables, which we take to be

$$W^2 = (k_1 + k_2)^2; \quad s = (K_1 + K_2 + \ldots)^2. \qquad (50)$$

We study the dependence of the amplitude on the variable s, for fixed W^2.

Let M denote the sum of the masses of the particles K_1 K_2,.... . The physical range of the variable s, for fixed W, is given by

$$M^2 < s < (W-m)^2 \equiv s_1 \qquad (51)$$

Now the triangle graph in question produces a normal threshold singularity at

$$s_n = (m_1 + m_2)^2 \quad . \tag{52}$$

If W is large enough, and if the internal particles are stable, as we assume, then the graph also produces an anomalous singularity. For $W > m_1 + m_3$ this occurs at the complex point $\bar{s}$ given by

$$\bar{s} = m_1^2 + m_2^2 - 2m_1 m_2 Z \tag{53}$$

where

$$Z = zz' + i\left[(z^2-1)(1-z'^2)\right]^{1/2} \tag{54}$$

$$z = \frac{m_1^2 + m_3^2 - W^2}{2m_1 m_3} \tag{55}$$

$$z' = \frac{m_2^2 + m_3^2 - m^2}{2m_2 m_3} \tag{56}$$

For $W = m_1 + m_3$, $\bar{s}$ is real and we have

$$\bar{s} - s_1 = (1 + m_1/m_3)\left[m_2^2 - (m_3 - m)^2\right] \tag{57}$$

$$s_n - \bar{s} = \frac{m_1}{m_3}\left[m^2 - (m_2 - m_3)\right]^2 \tag{58}$$

As W decreases below $m_1 + m_3$, $\bar{s}$ moves away from the physical region, toward the normal threshold. This is of course just what we do not want to happen, so we

shall not consider the case $W<m_1 + m_3$ any further.

However, we also note that the physical amplitude is obtained by allowing the variable s to approach the real axis from above, whereas for $W>m_1 + m_3$ the singularity $\bar{s}$ lies in the lower half s-plane. Thus the case where Re $\bar{s} \gg s_n$ is also uninteresting, since here a normal cut intervenes between s and $\bar{s}$ even when they are "close" to one another. Inspection of equations (53) to (57) shews that for $W \gg m_1 + m_3$ the singularity $\bar{s}$ moves far away from the physical region, except when $z' \backsim 1$; but in the latter case Re $\bar{s} \gg s_n$. All of these considerations therefore suggest that the most hppeful prospects for "detecting" the influence of the anomalous singularity corresponds to choosing W in a more or less narrow region near $m_1 + m_3$.

We can therefore most easily survey the possibilities by taking the simple case $W = m_1 + m_3$ and looking for diagrams for which $\bar{s} - s_1$ is small enough to be interesting, e.g. $\bar{s} - s_1 \lesssim$ (pion mass)^2.

Some examples are shewn in figure 23 and it is easy enough, by inspection of the equations, to generate others. All are somewhat impracticable in that they

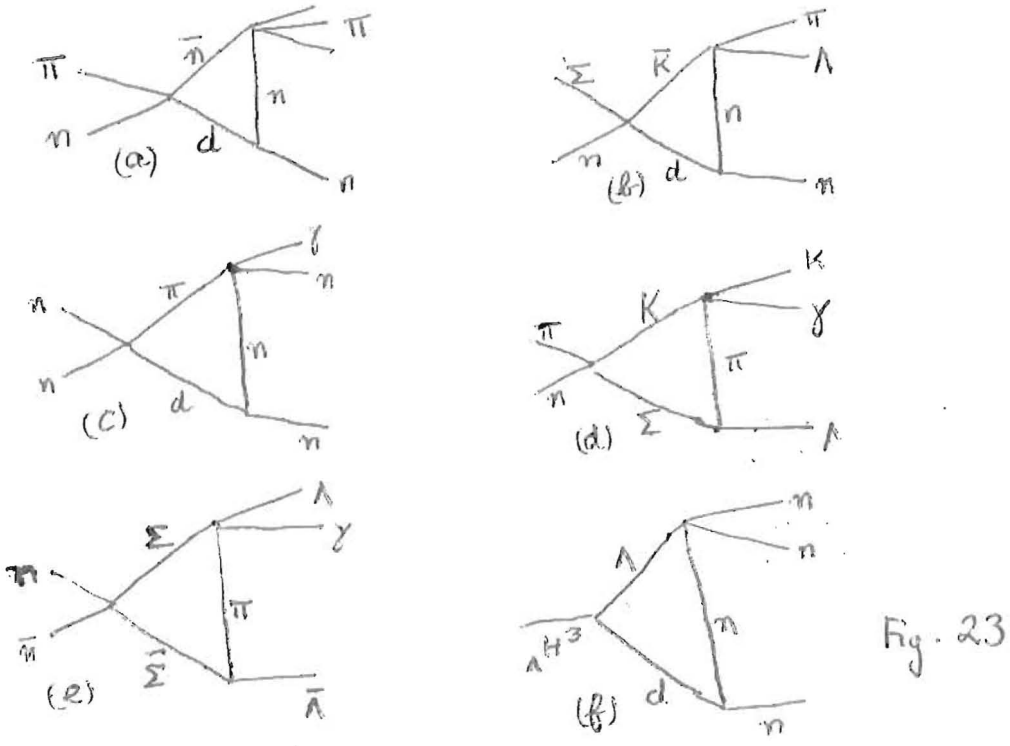

Fig. 23

involve emission of photons or require very high (and narrowly defined) incident particle energies or are concerned with processes that are as yet not very common. The sixth, a hyperfragment decay, involves a weak interaction. Notice that, in the notation of figure 22, the number and nature of the particles emitted at the (m_1, m_2) vertex is irrelevant in determining the location

of s_1 and $\bar{s}$, provided the choice is consistent with selection rules and, for given W, with energy-momentum conservation. Thus in figure 23a the particles emitted at the $(n, \bar{n})$ vertex could consist of any number of pions and, say, $K\bar{K}$ pairs, up to the limit set by available energy. Similarly, the nature of the incident particles in each graph has no effect on the location of the singularity. Thus, again in figure 23a, the incident $(\pi\ n)$ could be replaced by $(\bar{n}\ d)$. This might seem ideal for our purpose, since with our chosen value for W the antinucleon would be at rest, as is very convenient for experimental study. However, our triangle singularity $\bar{s}$ then coincides with the nucleon-exchange pole in the diagram obtained by 'dissolving' the $(\bar{n}\ d)$ interaction, so that our effect, although expected to be there, would be swamped by another*. The same remark applies to the hypertriton decay diagram of figure 23f if it is valid to regard the hypernucleus as a (Λd) scattering state. One might, however, say that this model should be modified by inclusion of the wave function for the Λ in the hypernucleus and that this could have the effect of changing the pole singularity precisely into one of the triangle

* This was pointed out by Dr. R. Blankenbecler

type.

We illustrate the way in which the anomalous singularity influences the transition amplitude by considering in detail one example, that of figure 23a. We compute the Feynman amplitude for this graph with neglect of structure effects at the vertices, since we are only concerned with the variation of the amplitude over a narrow range near the singularity. For the same reason we also neglect spin effects, treating all particles as spinless. A closed form for the Feynman integral has been obtained by A.C.T. Wu.[24] This contains a large number of Spence functions, however, and is unattractive for computation purposes. We prefer instead to write down a dispersion relation in the variable s. The weight function is easily obtained in explicit form, and the dispersion integral can readily be evaluated numerically. Details are set out in the Appendix.

The results are most conveniently expressed, not in terms of s, but rather in terms of a variable T which denotes the kinetic energy, in the overall center of mass system, of the outgoing nucleon. This

is related to the variables W and s by

$$T = \frac{S_1 - S}{2W}$$

For our simple choice W = + d (3 Bev) the transition amplitude is real and its dependence on T is shewn in figure 24. The sharp increase in the amplitude towards

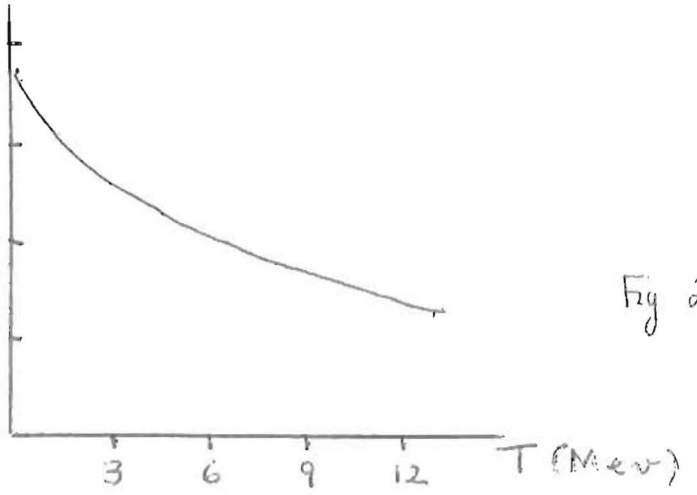

Fig 24

small T will be noted: the amplitude is roughly doubled in a width $\Delta T \approx 3$ Mev. In the region of rapid variation the squared amplitude varies as T^{-1}, an effect which should outweigh the phase volume effect, which goes as $T^{1/2}\, dT$. That is to say, insofar as the

graph in question dominates all others at small T, the experimental nucleon recoil spectrum should show a noticeable, narrow bump at small T. We may also remark here that, for fixed recoil nucleon energy T, our amplitude is independent of the angle of emission of the nucleon. This could be tested if one had reason to suspect that the graph in question were in fact dominating the reaction. Similar remarks hold for all the graphs under discussion.

The sharp effect indicated in figure 24 corresponds to the precise choice $W = n + d$. As W is increased, $\bar{s}$ becomes complex, but since z' is very nearly unity, ($z' = 1 - \epsilon$, $\epsilon \approx 1/800$), Im $\bar{s}$ remains small for a long while. However, Re $\bar{s}$ very quickly moves past the normal threshold at $4\,n^2$. By the time that W has increased by 50 Mev above the value n + d, all noticeable peak effects have disappeared, even though Re $\bar{s}$ and s_1 are very close to one another. As we have already said earlier, when the cut intervenes between $\bar{s}$ and a point s "near" to $\bar{s}$, the distance between the points must really be measured along a path that goes around the normal threshold, without crossing any cuts; that

distance increases rapidly here with increasing W.

We also learn in this example that there is no reason to suppose that only singularities that occur on what is usually taken to be the physical sheet should be effective. Singularities which are uncovered when the normal cuts are distorted may well be important if they lie near the physical region ("nearness" again somehow being defined in terms of a distance along a path that crosses no cuts). In fact this observation is relevant for the results of figure 24. The singularity at $\bar{s}$ is only logarithmic , so that one might have expected that no noticeable effect persist at s_1. What comes into play here, however, is the second type singularity at s_1, on the unphysical sheet reached through the cut attached to $\bar{s}$. It behaves as $1/(s_1-s)^{1/2}$ near s_1 and it combines with the logarithmic singularity at $\bar{s}$ in a subtle way to produce the sharp peaking effects noted here. How this comes about can be seen in more detail from the discussion given in the Appendix.

We note finally that the general character of the effects discussed above for the graph of figure 23a

holds also for the other graphs under consideration: a sharp peaking in the spectrum of the recoil particle at low energies, for incident energy W in a narrow interval near $m_1 + m_3$. The effect rapidly disappears with increasing energy W.

Appendix to Section 3.4

The weight functions in the representation for the triangle graph may be evaluated by the standard method of Cutkosky.[19] The result, when the singularity at $\bar{s}$ appears on the physical sheet, is proportional to

$$\int_{\bar{s}}^{s_n} \frac{2\pi}{\sqrt{K(s')}} \frac{ds'}{s'-s} + \int_{s_n}^{s_2} \frac{2}{\sqrt{K(s')}} \tan^{-1} \frac{\sqrt{K(s')L(s')}}{a(s')} \frac{ds'}{s'-s-i\epsilon}$$

$$+ \int_{s_2}^{\infty} \frac{i}{\sqrt{-K(s')}} \log \frac{a(s') + \sqrt{K(s')\,L(s')}}{a(s') - \sqrt{-K(s')\,L(s')}} \frac{ds'}{s'-s} \qquad (A1)$$

where

$$\begin{aligned} s_2 &= (W+m)^2 \\ K(s') &= (s_2 - s')(s' - s_1) \\ L(s') &= [s' - (m_1+m_2)^2][s' - (m_1-m_2)^2] \\ a(s') &= s'^2 + s'(2m_3^2 - m_1^2 - m_2^2 - W^2 - m^2) \\ &\quad + (W^2 - m^2)(m_1^2 - m_2^2) \end{aligned} \qquad (A2)$$

and s_1, s_n, $\bar{s}$ are defined respectively in (51), (52), (53).

We have written (A1) in the form directly applicable to our computation discussed in section 3.4, where we took $W = m_1 + m_3$ so that $\bar{s}$ was real and $s_1 < s_n$. In this case the square roots in (A1) are to be taken to have positive values and the logarithm is real. The arctangent takes the value π at s_n' and 0 at s_2', there being a zero of $a(s')$ in between these points. The first integral in (A1) may be evaluated in closed form and the result is

$$\frac{4\pi}{\sqrt{-K(s)}}\left[\tan^{-1}\sqrt{\frac{(s_n-s_1)(s_2-s)}{(s_2-s_n)(s_1-s)}}-\tan^{-1}\sqrt{\frac{(\bar{s}-s_1)(s_2-s)}{(s_2-\bar{s})(s_1-s)}}\right] \qquad (A3)$$

where again the radicals are positive and the arctangents lie between 0 and π. The remaining two integrals in (A1) must be estimated numerically.

When $s_1 > s_n$ and when $\bar{s}$ is complex the equations (A1) and (A3) are still formally correct. The sheets of the logarithm and arctangents must be determined by continuation from the previous case.

We may notice some qualitative features of our function for the case discussed in section 3.4. The value of (A3) at $s = s_1$ is

$$\frac{4\pi}{s_2 - s_1}\left[\left(\frac{s_2 - \bar{s}}{\bar{s} - s_1}\right)^{1/2} - \left(\frac{s_2 - s_n}{s_n - s_1}\right)^{1/2}\right] \qquad (A4)$$

When, as in our case, $\bar{s}$ and s_1 are close together this is large. The second integral in (A1) produces a contribution of the same order of magnitude.

As s is taken below s_1 the contribution (A3) falls off rapidly, both because -K(s) increases and because the arctangents become nearly equal. The second integral, however, falls off more slowly. a(s') has a zero at a point s^* close to s_n and a substantial part of the contribution from the second integral arises from the range s^* to about $2s^*$. A crude idea of the behaviour may be obtained by approximating the arctangent as $\pi/2$ in this range and then the result of the integration is as in (A3), with s_n replaced by $2s^*$ and $\bar{s}$ by s_n. As S varies over a small range below s_1, the arctangents are sensibly constant and so we see that the behaviour is as $1/\sqrt{s_1 - s}$. This is in accord with our assertions in section 3.4 concerning the interplay of the singularity at $\bar{s}$ with the second typesingularity at s_1. The effect of the nearness of

the $\bar{s}$ singularity is mainly felt indirectly in that it causes the zero s^* of $a(s)$ to be close to s_n.

References

Reviews of much of the work described here are to be found in the lectures of J. C. Polkinghorne at the Edinburgh Summer School (1960), of R. J. Eden at Maryland University (1961), of R. J. Eden and of J. C. Polkinghorne at Brandeis University Summer School (1961) and in a forthcoming review article by R. J. Eden. See also the Proceedings of the conferences on high energy physics at Rochester (1960) and at La Jolla (1961).

References cited in the text:-

1. P. V. Landshoff, Nuclear Physics 20, 129 (1960)
2. M. Fowler, P. V. Landshoff and R. W. Lardner, Nuov. Cim. 17, 956 (1960)
3. P. V. Landshoff, J. C. Polkinghorne and J. C. Taylor, Nuov. Cim. 19, 939 (1961)
4. R. J. Eden, P. V. Landshoff, J. C. Polkinghorne and J. C. Taylor, Phys. Rev. 122, 307 (1961)
5. P. V. Landshoff and S. B. Treiman, Nuov. Cim. 19, 1249 (1961)
6. R. J. Eden, P. V. Landshoff, J. C. Polkinghorne and J. C. Taylor, J. Math. Phys. 2, 656 (1961)
7. D. B. Fairlie, P. V. Landshoff, J. Nuttall and J. C. Polkinghorne, J. Math. Phys. To be published.
8. P. V. Landshoff and S. B. Treiman, Phys. Rev. To be published.
9. G. Kallen and A. S. Wightman, Dan. Vid. Selsk. Mat-fys. Skr. 1, No. 6 (1958)

10. R. Karplus, C. M. Sommerfield and E. H. Wichmann, Phys. Rev. 111, 1187 (1958)
11. J. C. Polkinghorne, preprint; H. Stapp, preprint
12. J. Hadamard, Acta Math. 22, 55 (1898). This lemma was first used in quantum field theory by R. J. Eden, Proc. Roy. Soc. A 210, 388 (1952) and further developed by J. C. Polkinghorne and G. R. Screaton, Nuov. Cim. 15, 289 (1960).
13. L. D. Landau, Nuclear Physics 13, 181 (1959). J. C. Taylor, Phys. Rev. 117, 261,(1960)
14. S. Mandelstam, Phys. Rev. 112, 1344 (1958)
15. A. C. T. Wu, Dan. Vid. Selsk. Mat-fys. Skr.
16. G. Kallen and H. Wilhelmsson, Dan. Vid. Selsk. Mat-fys, Skr. 1, 9 (1959)
17. K. Symanzik, Prog. Theor. Phys. 20, 690 (1958)
18. J. Tarski, J. Math. Phys. 1, 154 (1960)
19. R. Cutkosky, J. Math. Phys. 1, 429 (1960)
20. J. C. Polkinghorne and G. R. Screaton, Nuov. Cim. 15, 925 (1960)
21. S. Mandelstam, Phys. Rev. 112, 1344 (1958)
22. R. J. Eden, Phys. Rev. 119, 1763 and 121, 1566 (1960)
23. G. F. Chew and F. E. Low, Phys. Rev. 113, 1640 (1959)
24. A. C. T. Wu, private communication.